Electronic Supplementary Information (ESI) for:

Photoswitching Activation of a Ferrocenyl-Stilbene Analogue by its Covalent Grafting to Gold

Francesc Bejarano,[a] Diego Gutiérrez,[a,b] José Catalán-Toledo,[a] Daniel Roca-Sanjuán,[c] Johannes Gierschner,*[d] Jaume Veciana, [a] Marta Mas-Torrent, [a] Concepció Rovira, Núria Crivillers*[a]

Email: ncrivillers@icmab.es

1. Solvents and reagents

All the commercial electrolytic salts and reagents were purchased from Sigma-Aldrich and used without further purification. Synthesis grade solvents employed in synthesis and column chromatography, were purchased from Scharlab, Sigma-Aldrich or Carlo Erba. HPLC grade solvents were purchased from Scharlab or Teknokroma, and spectroscopic grade solvents, from Teknokroma. Deuterated solvents used for NMR characterization were purchased from Eurisotop. Both HPLC and deuterated solvents were used without further treatment. 6-(Ferrocenyl)hexanethiol was purchased from Sigma-Aldrich and used without further purification.

2. Apparatus and techniques

2.1 Nuclear Magnetic Resonance (NMR) spectroscopy: The ^{1}H NMR and ^{13}C NMR spectra were registered on a Bruker Avance-III 400 MHz spectrometer (9.4 T) with a BBFO probe that permits different nuclei acquisition and automatic tuning and with an HR-MAS accessory for high-resolution NMR. Samples were prepared in deuterated dichloromethane (CD_2Cl_2) or deuterated chloroform ($CDCl_3$). All spectra are calibrated using residual undeuterated dichloromethane ($\delta(1H) = 5.32$ ppm; $\delta(13C) = 53.84$ ppm) and residual undeuterated chloroform (δ(1H) = 7.26 ppm; δ(13C) = 77.00 ppm) as internal references. The data analysis was carried out with MestReNova soft-ware (MestReLab Research S. L.). The following abbreviations are used to designate multiplicities: br = broad signal, s = singlet, d = doublet, t = triplet, m = multiplet. Other abbreviations used are: xJ = coupling constant at X bonds of distance, ArC = aromatic carbon).

2.2 Electrochemical characterization: Cyclic Voltammetry (CV): The CVs were performed in a standard cell with an AUTOLAB 204 with NOVA 1.9 soft-ware. A 0.1 or 0.2 M solution of tetra-n-butylammonium tetrafluoroborate ($TBAPF_6$) in THF, ACN or CH_2Cl_2 was employed as electrolyte and a platinum wire as counter electrode. The working electrode was a platinum wire for the solution analysis and, for the surfaces characterization, the modified metallic electrode (gold) itself. A home-made PTFE electrochemical cell was used. This cell permitted a proper estimation of the analyzed area (0.50 cm^2). Ag/AgCl commercial electrode, a polished Ag wire or ferrocene in solution were selected as reference electrodes or internal reference depending on the studied sample.

2.3 Infrared (IR) spectroscopy: IR spectra were registered with a FT-IR PerkinElmer spectrometer with a diamond ATR accessory, upon at least 6 scans, and background-corrected. The following abbreviations are used to indicate the relative intensity of the signals: s = strong, m = medium, w = weak.

2.4 Ultraviolet-visible (UV-vis) absorption spectroscopy: UV-vis absorption spectra were registered on a Varian Cary 5000 UV-Vis-NIR spectrometer. Quartz cuvettes with an optical path of 1 cm were used.

2.5 Matrix-Assisted Laser Desorption/Ionization – Time of Flight (MALDI-ToF) mass spectrometry: Spectra were registered on a Bruker Ultraflex mass spectrometer by operating at ion pulsed extraction at high power.

2.6 X-ray Photoelectron Spectroscopy (XPS): XPS measurements were performed with a Phoibos 150 analyzer (SPECS GmbH, Ber-lin, Germany) in ultra-high vacuum conditions (base pressure 5·10-10 mbar) with a mon-ochromatic aluminum K-alpha X-ray source (1486.74 eV). The energy resolution as measured by the FWHM of the Ag 3d5/2 peak for a sputtered silver foil was 0.58 eV.

2.7 Photoisomerization experiments: An Oriel model 68911 500 W Arc Lamp Power Supply coupled to a DC Xe and Hg(Xe) arc lamp light was used. The light beam was guided and focused onto the samples by a bendable optical fiber connected to the lamp. A monochromator was placed in the channel between the lamp and the optical fiber when selective wavelength irradiation was performed. For all the experiments, the employed solvents were of HPLC quality and the incident power on the sample was measured with a powermeter from Thorlabs. UV irradiation experiments (λ=254 nm) were performed with a handheld UV lamp from Company Seven and UVP. In the case of the SAMs, the lamp was placed 15 cm far from the substrate.

2.8 Statistical Analysis of the measured IV curves: For the statistical analysis of the I-V curves, we have employed the free R software. For doing so, we have taken into account that the trimmed mean values and standard deviations are robust estimators of central tendency. To compute a trimmed mean, a predetermined amount of observations is removed on each side of a distribution (remove outliers), and average the remaining observations. Trimmed mean values provide a better estimation of the location of the bulk of the observations than a bare mean function when sampling from slightly asymmetric distributions. On the other hand, the bare standard deviation is dramatically affected by outliers and slightly asymmetries. More reliable results are obtained using the trimmed standard deviation. The trim argument can vary between 0 and 0.5. In this work, we have removed 10% of the total data, for which trim argument must be equal to 0.1. In this case, 5% of the upper part and 5% in the lower part is omitted.

3. Surface coverage determination

The average surface coverage is determined using the following equation

$$\theta = Q/nF(Sr)$$

θ is the surface coverage of the SAM (in mol per area unit), n is the number of electrons involved in the redox process (one, in this case), Sr is the scan rate applied and Q is the charge estimated from the area under either the anodic or the cathodic voltammetry peak without taking into account the capacitive current.

4. Synthesis of *trans*-1 and *cis*-1

Synthesis of (4-ethynylbenzyl)triphenylphosphonium bromide ***(2):*** In a round-bottom flask, 1-(bromomethyl)-4-ethynylbenzene (657 mg, 5.1 mmol) and triphenylphosphine (2.133 g, 8.1 mmol) were dissolved in benzene (80 mL). The reaction mixture was stirred under reflux for 5 hours. The resulting suspension was poured onto 100 mL of benzene and filtered under vacuum to afford the product as a white solid (1.386 g, 69% yield). ^{1}H NMR (400 MHz, $CDCl_3$, δ): 7.78 (m, 9H, ArC-**H**), 7.63 (d, 6H, ArC-**H**), 5.56 (d, 2H, ^2J(P-H) = 8.4 Hz, C$\mathbf{H_2}$), 3.08 (d, 1H, ^8J(P-H) = 1.0 Hz, CΞC-**H**) ppm, **LDI-ToF** (positive mode): *m/z* 377.1 [M – Br].

*Synthesis of 1-ferrocene-2-(4-ethynylphenyl)ethene (**trans-1**) and (**cis-1**):* Compound **1** was obtained through a Wittig reaction. Compound **2** (507 mg, 1.11 mmol) was dissolved in anhydrous THF (20 mL) under N_2 atmosphere. Potassium *tert*-butoxide

(196 mg, 1.75 mmol, 1.6 eq) was added to the resulting white suspension, which gradually turned to orange. 20 minutes later, a solution of ferrocenecarboxaldehyde (479 mg, 2.24 mmol, 2.0 eq) in anhydrous THF (3 mL) was added dropwise and the reaction mixture was protected from light and stirred overnight. Then, the reaction was quenched upon diluted HCl addition until slightly acidic pH was achieved. CH_2Cl_2 (20 mL) and water (20 mL) were added and the two phases were separated. The aqueous layer was extracted with more CH_2Cl_2 (3 x 15 mL). The combined organic phases were dried over anhydrous Na_2SO_4, filtered and concentrated under vacuum to afford an orange crude which was purified by column chromatography (SiO_2, hexanes/ CH_2Cl_2 8:2) giving 15 mg of pure *trans* isomer, 96 mg of pure *cis* isomer and 220 mg of *cis*/*trans* mixture (total yield 92%). The isomeric mixture was converted to almost pure *trans* isomer after refluxing it in toluene with I_2 (0.05 eq) overnight and washing it with an aqueous saturated solution of $Na_2S_2O_3$ until no iodine was observed (orange color) in the aqueous phase. After that, the organic layer was dried over anhydrous Na_2SO_4, filtered and concentrated under vacuum, giving rise to an orange solid which was recrystallized in hexane/dichloromethane 9:1 affording red crystals of pure *trans* isomer with needle shape. ***1-trans***: ^{1}H NMR (400 MHz, CD_2Cl_2, δ): 7.44 (d, ^3J = 8.4 Hz, 2H, ArC-**H**), 7.39 (d, ^3J = 8.4 Hz, 2H, ArC-**H**), 6.94 (d, ^3J = 16.2 Hz, 1H, H-C=C-**H**), 6.68 (d, ^3J = 16.2 Hz, 1H, **H**-C=C-H), 4.50 (t, ^3J = 1.7 Hz, 2H, Fe-C_5-$\mathbf{H_2}$ **(a)**), 4.32 (t, ^3J = 1.7 Hz, 2H, Fe-C_5-$\mathbf{H_2}$ **(b)**), 4.15 (s, 5H, Fe-C_5-$\mathbf{H_2}$), 3.17 (s, 1H, C≡C-**H**) ppm; ^{13}C NMR (101 MHz, CD_2Cl_2, δ): 138.99 (ArC), 132.76 (ArC-H), 129.16 (**C**=C), 125.98 (ArC-H), 125.31 (C=**C**), 120.31 (Ar**C**-C≡C), 84.16 (**C**≡C-H), 83.43 (Fe-**C**-C=C), 77.78 (C≡**C**-H), 69.85 (Fe-**C**-H_2 **(a)**), 69.75 (Fe-**C**-H_2), 67.51 (Fe-**C**-H_2 **(b)**) ppm; ATR-IR: ν (cm^{-1}) = 3304 (m) (C≡C-H), 3262 (w), 3110 (w) , 3098 (w) , 3077 (w) , 3029 (w) (ArC-H), 2101 (w) (C≡C), 2052 (w), 1966 (w), 1932 (w), 1910 (w), 1828 (w), 1784 (w), 1777 (w),

1764 (w), 1698 (w) , 1634 (m) , 1598 (m) , 1552 (w) (ArC-ArC), 1506 (m) (ArC-ArC), 1488 (w), 1463 (w), 1411 (w) , 1393 (w), 1376 (w), 1360 (w) , 1348 (w), 1293 (w), 1254 (sh, m) , 1244 (m), 1204 (w), 1172 (w), 1107 (m) , 1060 (w), 1042 (m), 1026 (m), 1000 (m) , 969 (m), 961 (m), 948 (m), 931 (m), 897 (w), 862 (m), 827 (m), 810 (s) , 763 (w), 725 (w), 697 (w), 673 (s), 645 (m), 624 (s); LDI-ToF (positive mode): *m/z* 312.0 [M] ; UV-vis (ACN) λ_{max} (ε): 197 (45843), 219 (16956), 275 (14486), 322 (30655), 380 (2723), 461 nm (1918); **CV** (0.1 M $TBAPF_6$ in ACN, vs Ag/AgCl): $E^{1/2}$ = 0.44 V. ***1-cis*:** ^{1}H NMR (400 MHz, CD_2Cl_2, δ): 7.41 (d, ^3J = 8.3 Hz, 2H, ArC-**H**), 7.30 (d, ^3J = 8.3 Hz, 2H, ArC-**H**), 6.39 (d, ^3J = 12 Hz, 1H, H-C=C-**H**), 6.34 (d, ^3J = 12 Hz, 1H, **H**-C=C-H), 4.17 (m, 4H, Fe-C_5-**H_2 (a) and (b)**), 4.10 (s, 5H, Fe-C_5-**H_2**), 3.09 (s, 1H, C≡C-**H**) ppm; ^{13}C NMR (101 MHz, CD_2Cl_2, δ): 138.90 (Ar**C**-C=C), 131.83 (ArC-H), 129.25 (**C**=C), 128.67 (ArC-H), 126.33 (C=**C**), 120.05 (Ar**C**-C≡C), 83.88 (**C**≡C-H), 81.13 (Fe-**C**-C=C), 77.17 (C≡**C**-H), 69.52 (Fe-**C**-H_2 **(a)**), 69.36 (Fe-**C**-H_2), 68.81 (Fe-**C**-H_2 **(b)**) ppm; ATR-IR: ν (cm^{-1}) = 3263 (m) (C≡C-H), 3247 (sh, m), 3095 (w) , 3078 (w) , 3014 (w) (ArC-H), 2103 (w) (C≡C), 2021 (w), 1992 (w), 1727 (w) , 1627 (sh,w) , 1622 (w) , 1600 (w), 1548 (w) (ArC-ArC), 1506 (sh, w) (ArC-ArC), 1500 (w), 1465 (w), 1412 (w), 1403 (w) , 1387 (w), 1371 (w) , 1347 (w), 1270 (m), 1254 (w) , 1216 (w), 1196 (w), 1178 (w), 1156 (w), 1104 (m) , 1081 (w), 1063 (w), 1052 (w), 1037 (w), 1027 (m), 999 (m) , 968 (w), 959 (w), 927 (w), 857 (m) , 830 (m), 815 (s) , 787 (sh, m) , 762 (m), 748 (m), 728 (m), 673 (s), 665 (sh, m), 649 (sh, w), 638 (s), 629 (sh, m), 591 (w), 585 (w), 574 (w), 569 (w); LDI-ToF (positive mode): *m/z* 312.0 [M] ; UV-vis (ACN) λ_{max} (ε): 200 (49110), 224 (23468), 275 (14473), 305 (14647), 371 (2052), 448 nm (805); **CV** (0.1 M $TBAPF_6$ in ACN, vs Ag/AgCl): $E^{1/2}$ = 0.46 V

5. Additional figures

<u>UV-vis of the *cis-trans* isomerization in solution (**Fig. S1 and S2 below**):</u>

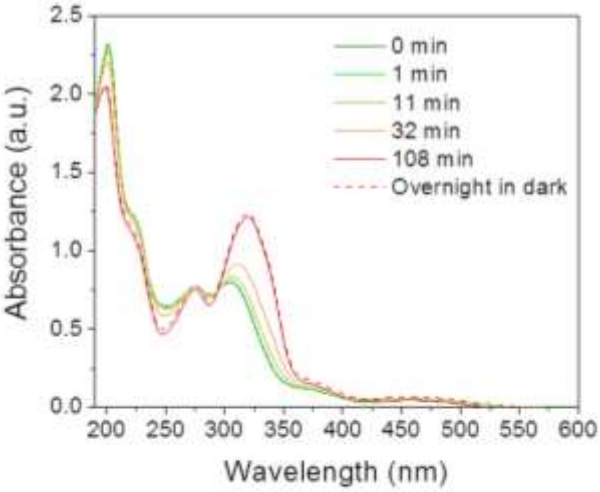

Fig. S1. UV-vis spectra evolution of ***cis-1*** (0.053 mᴍ in acetonitrile) irradiated at λ=254 nm (~700 mW)

An initial attempt to study the *trans*→cis photoisomerization was performed by irradiating a 1.5 mᴍ solution of ***trans-1*** in methanol at λ=366 nm (incident power ~340 mW). The evolution was followed by both UV-vis and HPLC means, but any sign of isomerization was observed. Further attempts were carried out to photoisomerize ***trans-1***. First, the same experiment was repeated decreasing concentrations to 0.1 mᴍ, as well as in acetonitrile (Figure S2) and finally, at 0.0043 mᴍ in *n*-pentane, following conditions similar to experiments found in literature for a *trans*→*cis* stilbene photoisomerization. The interconversion process failed. With the idea of moving to a higher-absorption spectral window and to increase the photoyield, the irradiation source was replaced by an arc lamp with a 340 nm filter and an optical fiber to illuminate the sample, but it was unsuccessful.

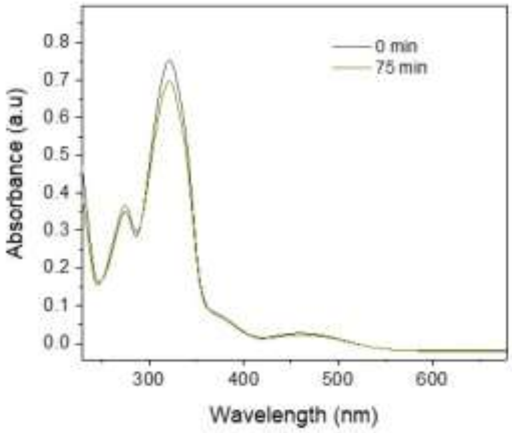

Fig. S2. UV-vis spectra evolution of ***trans-1*** (in acetonitrile) irradiated at λ=366 nm.

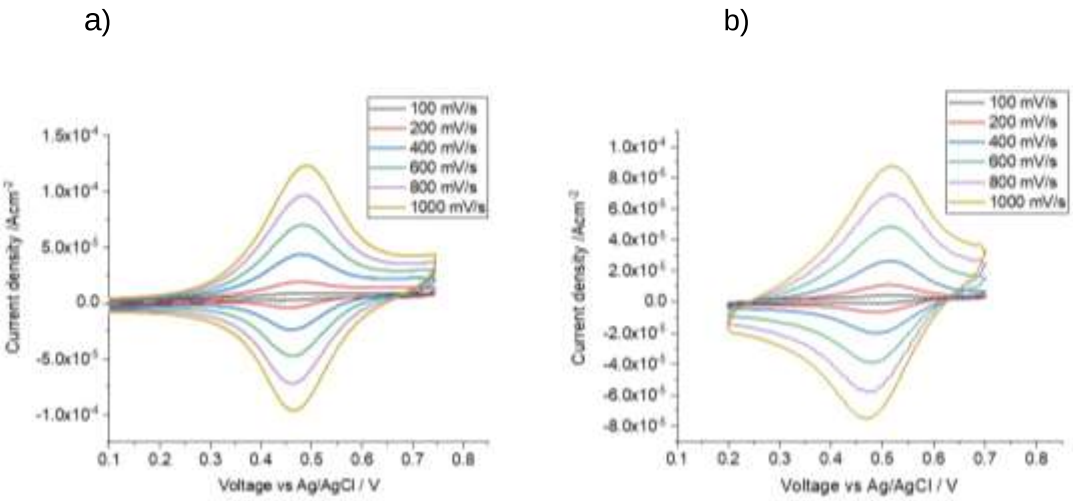

Fig. S3. Cyclic voltammogram of the a) ***trans-1*-SAM** and b) **the *cis-1*-SAM**. Using $TBAPF_6$ in ACN (0.1M) as supporting electrolyte. SAM/Au is used as WE, Ag/AgCl(sat) as RE and Pt wire as CE.

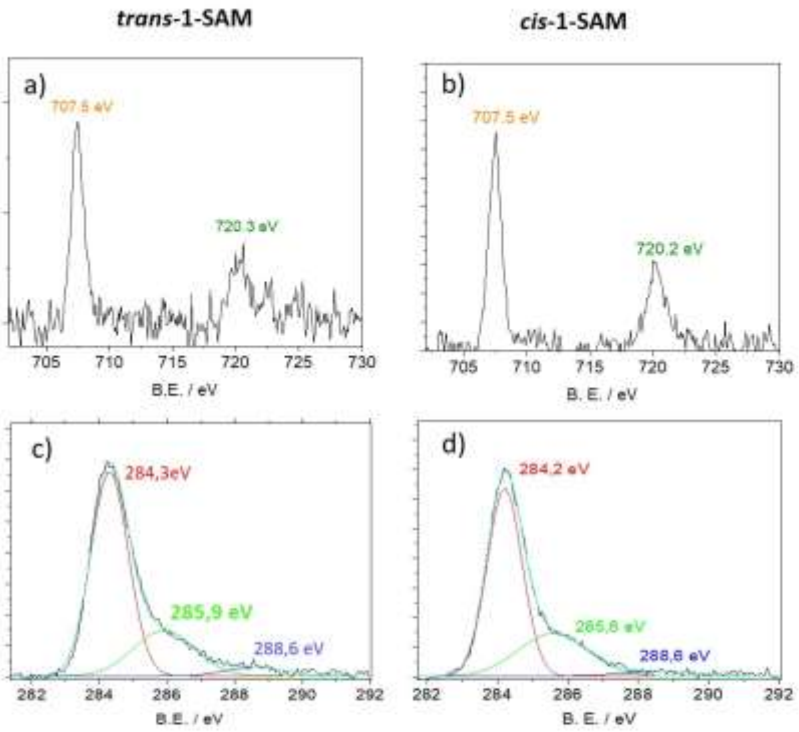

Fig. S4. Fe2p (a and b) and C1s (c and d) XPS spectra of the ***trans*-** and ***cis*-1-SAM**

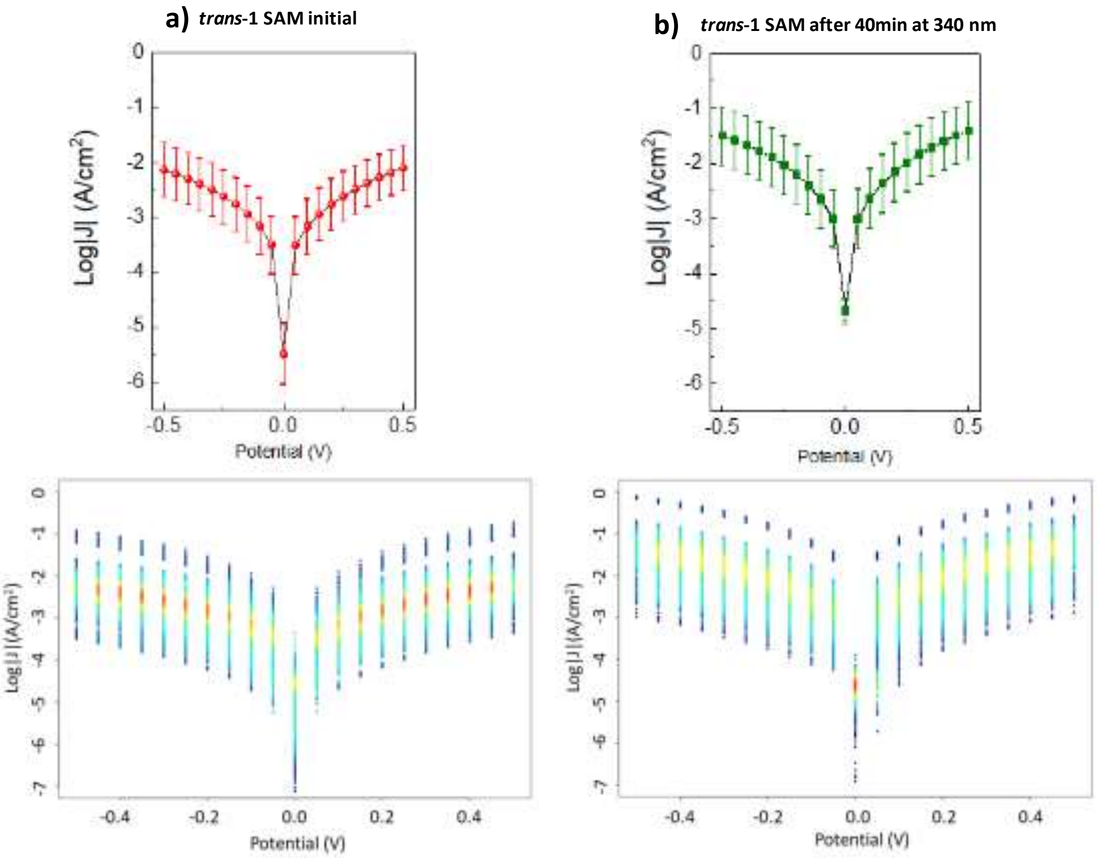

Fig. S5. a) Top: JVs plot acquired for ***trans*-1-SAM**; Bottom: Corresponding heatmap plot. b) Top: JV plot for ***trans*-1-SAM after 40 minutes of irradiation at 340nm;** Bottom: Corresponding heatmap plot. For top graphs, dots (circles and squares) indicate mean values while the bars stand for the standard deviation. Data collected (before irradiation): 760 curves, 65 junctions with junction yield formation of 81%.

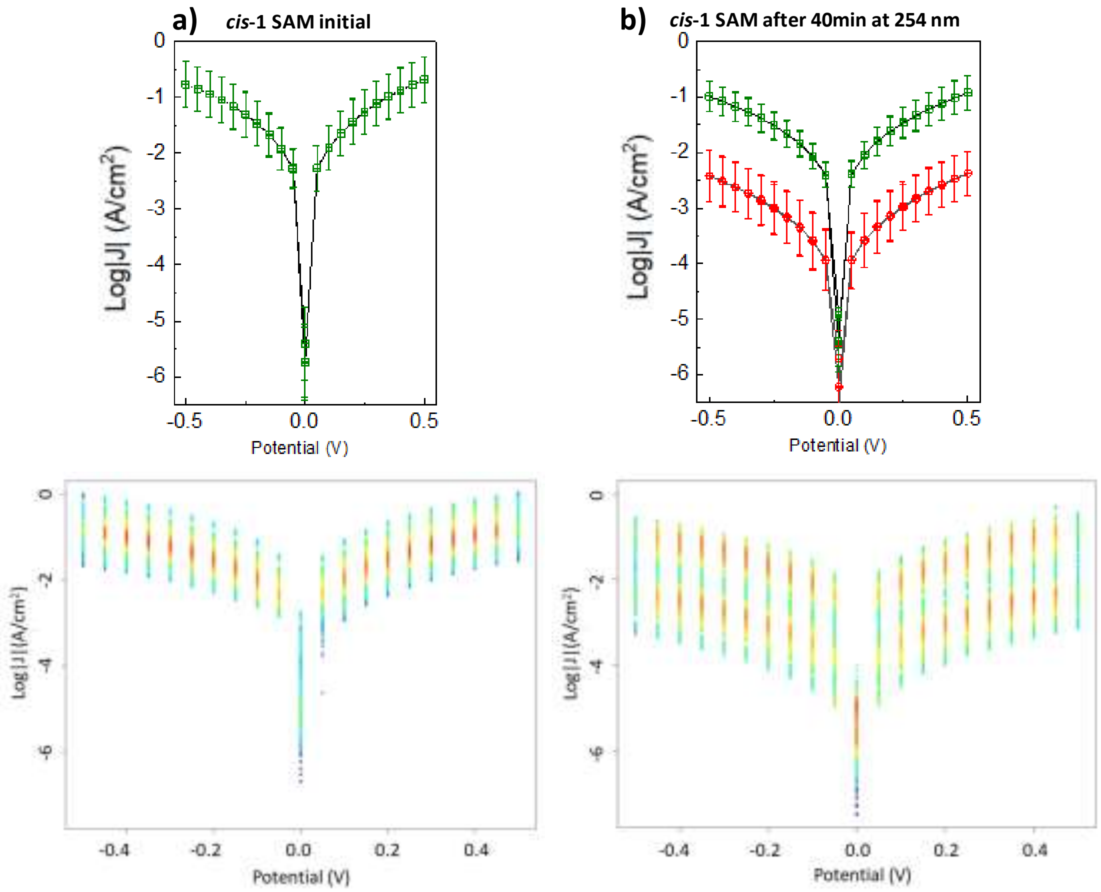

Fig. S6. a) Top: JVs plot acquired for ***cis*-1-SAM**; Bottom: Corresponding heatmap plot. b) Top: JV plot for ***cis*-1-SAM after 40 minutes irradiation at 254 nm;** Bottom: Corresponding heatmap plot. For top graphs, dots (circles and squares) indicate mean values while the bars stand for the standard deviation. Data collected (before irradiation): 264 curves, 22 junctions with junction yield formation of 78%.

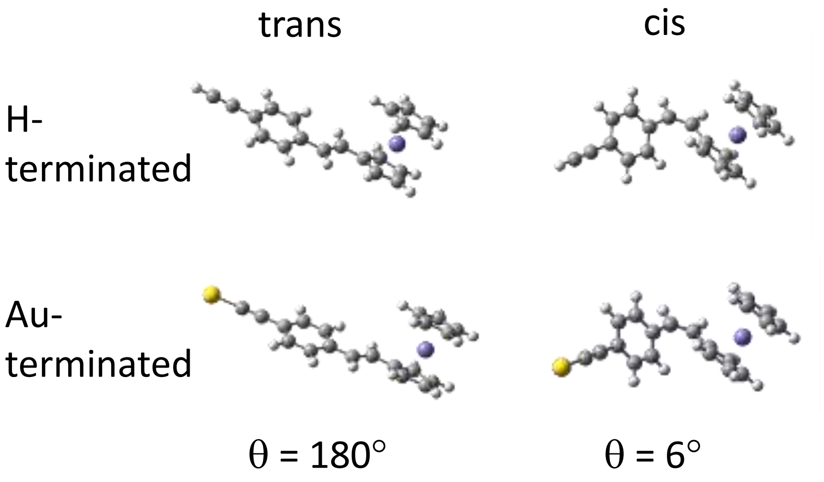

Fig. S7. a) DFT-optimized structures of the H- and Au-terminated compounds in the *trans*- and *cis*-conformation with dihedral angles.

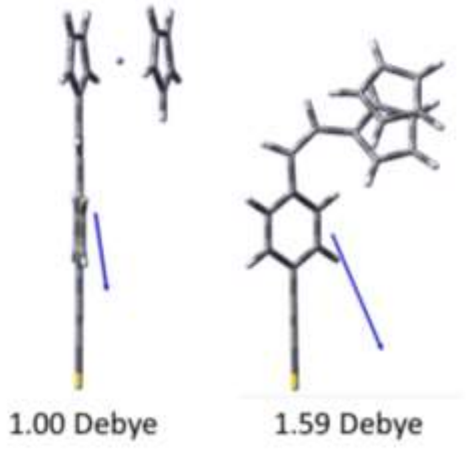

Fig. S8. CDFT-calculated static dipole moments of the trans- and cis isomers for the Au-terminated compounds.

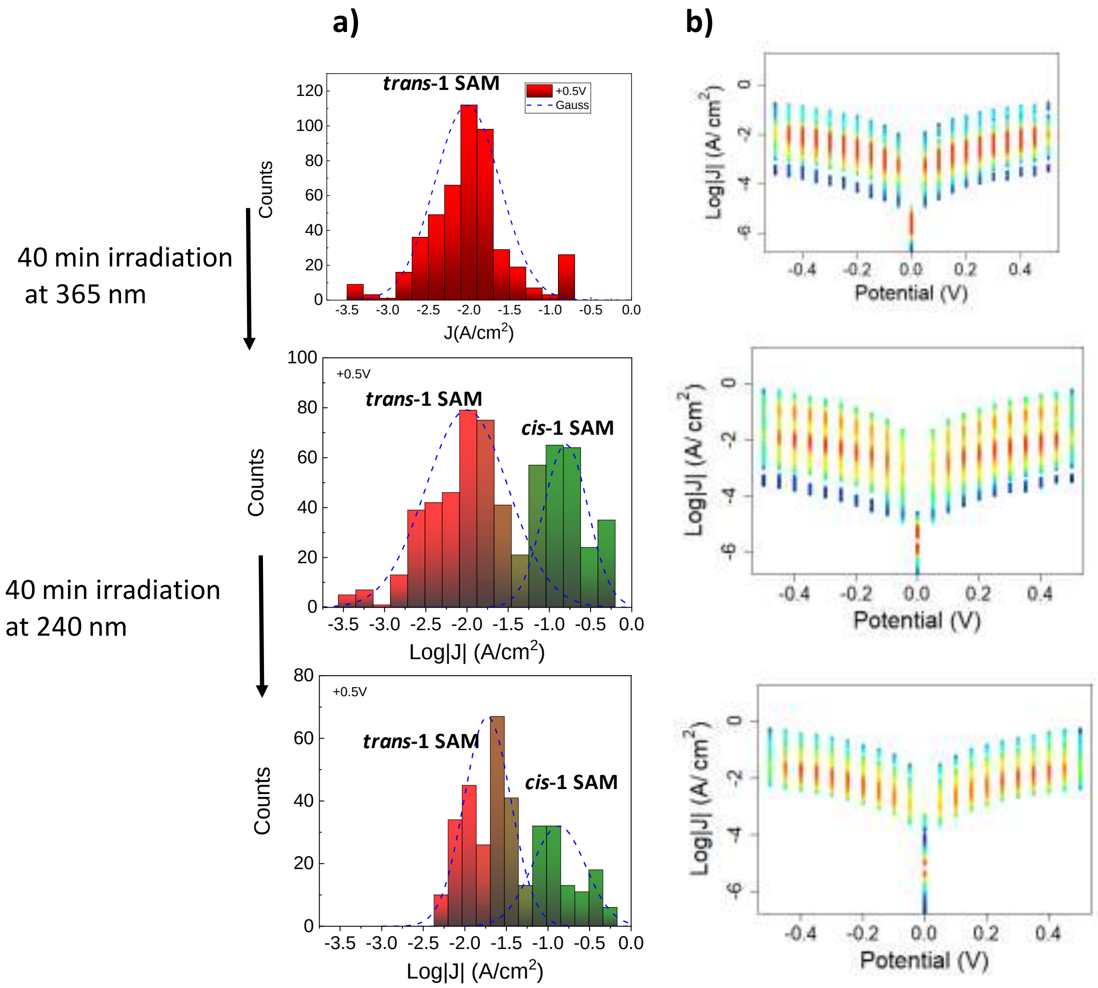

Fig. S9. a) Histogram of log |J| at +0.5 V for ***trans*-1-SAM** before (top), after 40 minutes of irradiation at 365 nm (middle) and after 40 minutes of irradiation at 240nm. The data collection is separated in two distinct populations. b) Heatmap plots for each irradiation step.

Blank experiment: 6-(Ferrocenyl)hexanethiol (FcC_6SH). A Au^{TS} was immersed in a 0.5 mM solution in ethanol for 24hours at room temperature. The substrate was then rinsed with ethanol and dried under nitrogen. The FcC_6S-Au^{TS} were measured immediately after the preparation.

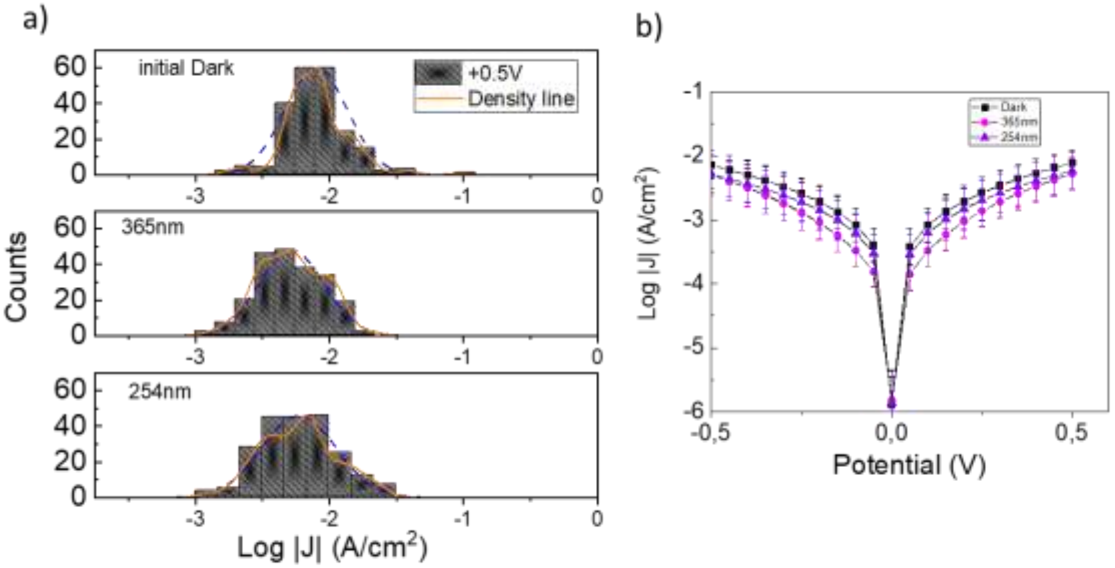

Fig. S10. a) Histogram of Log |J| for the EGaIn/Ga_2O_3//FcC_6S//Au^{TS} junction, before and after irradiation with a lamp of 365 nm and 254 nm for 40 minutes each experiment. b) Corresponding *JV* curves for each experiment shown in a).

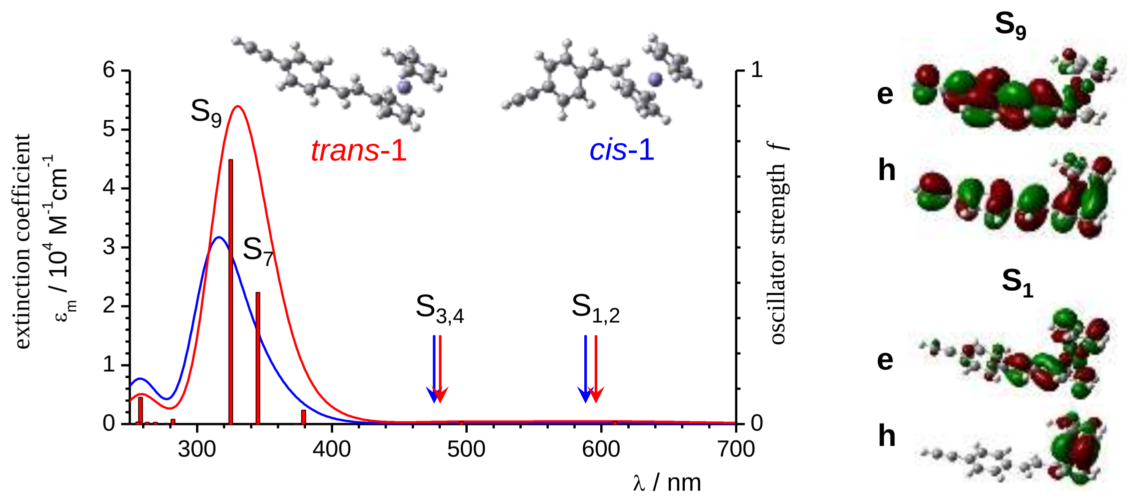

Fig. S11. TD-DFT (B3LYP) calculated electronic absorption spectra of ***trans*-1** (red) and ***cis*-1** (blue) obtained in a single point approach, broadened by Gaussians of 0.25 eV width. For ***trans*-1**, also the stick spectrum is given, and the associated natural transition orbitals (NTOs; with h = hole, e = electron) for S_1 and S_9 on the right side.

Table S1: TD-DFT (B3LYP) calculated properties for the *trans*- and *cis*-isomers of the different compounds in the ground (S_0) and lowest excited singlet state (S_1) and triplet (T_1) states. Bond length d_{DB} of the vinyl double bond (in Å). Vertical and adiabatic transition energies E_{vert}, E_{adiab}, given (in eV) with respect to their respective (*trans*/*cis*) S_0; relative energies of the ground state *cis*-isomers vs. *trans* are 0.15 eV for **StFc**, 0.17 eV for **1**, and 0.17 eV for **1-Au**.

comound	isomer	d_{DB}			E_{vert}		E_{adiab}	
		S_0	S_1	T_1	S_1	T_1	S_1	T_1
StFc	*trans*	1.345	1.347	1.347	2.01	1.06	1.44	0.57
	cis	1.346	1.348	1.347	2.06	1.14	1.48	0.60
1	*trans*	1.346	1.349	1.348	2.03	1.13	1.46	0.77
	cis	1.347	1.349		2.06	1.14	1.48	
1-Au	*trans*	1.346	1.372	1.347	1.67	1.10	1.39	0.59
	cis	1.347	1.376	1.348	1.76	1.14	1.45	0.60

ANEX I: ^{1}H-NMR, ^{13}C-NMR, FT-IR and LDI-ToF data

a) Compound ***trans*-1**

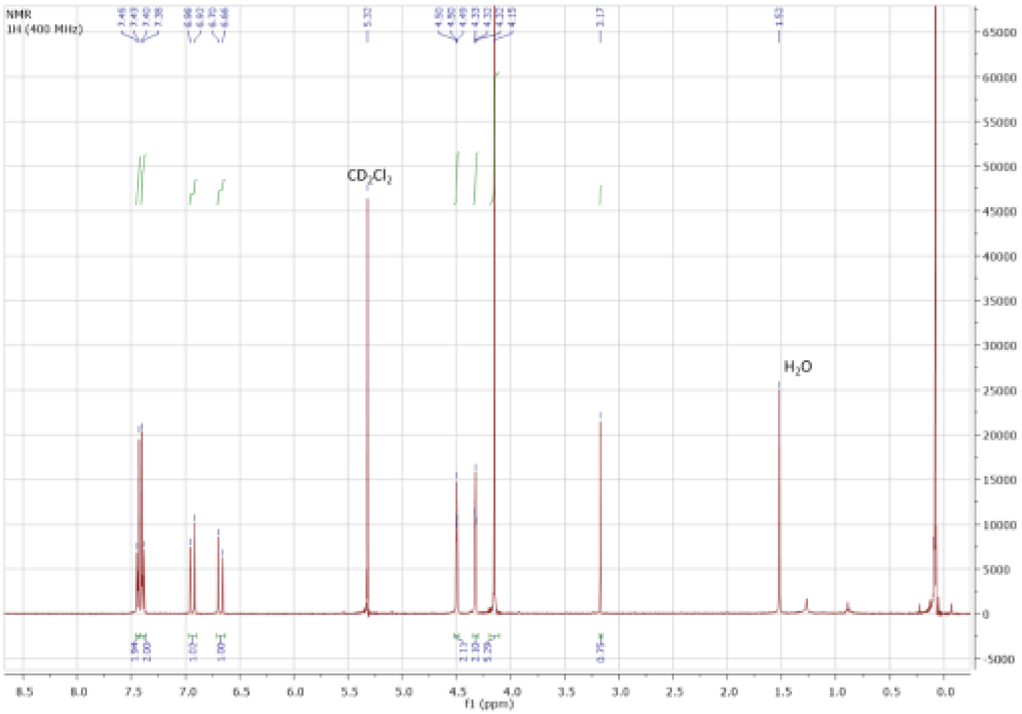

Fig. S12. ^{1}H-NMR spectrum of compound ***trans*-1** in CD$_2$Cl$_2$.

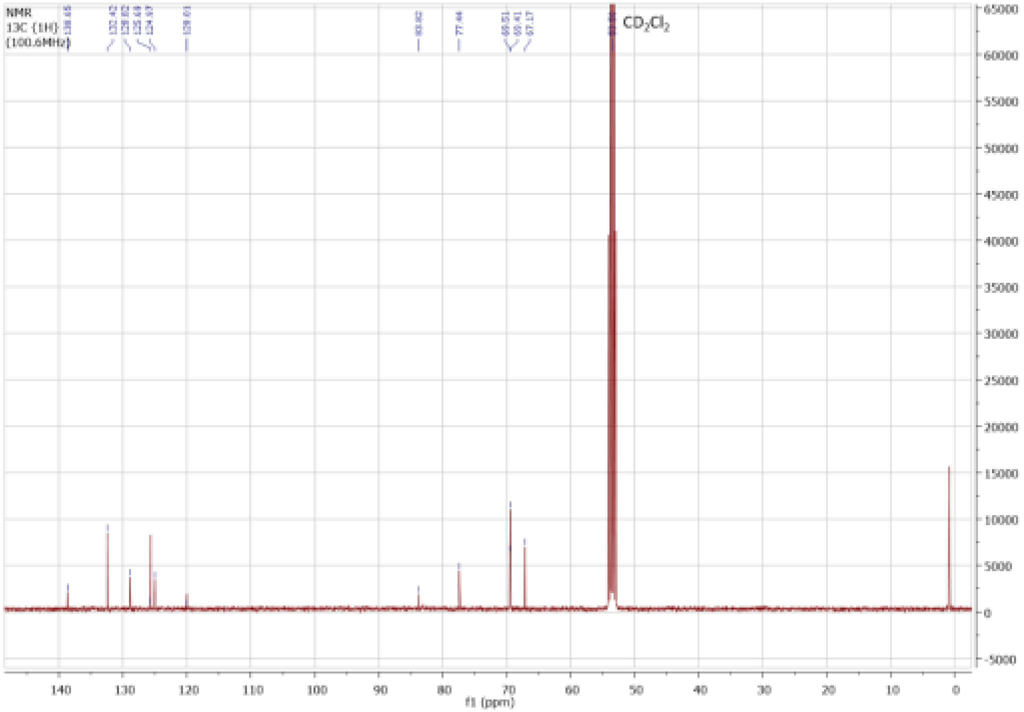

Fig. S13. ^{13}C-NMR spectrum of compound ***trans*-1** in CD_2Cl_2.

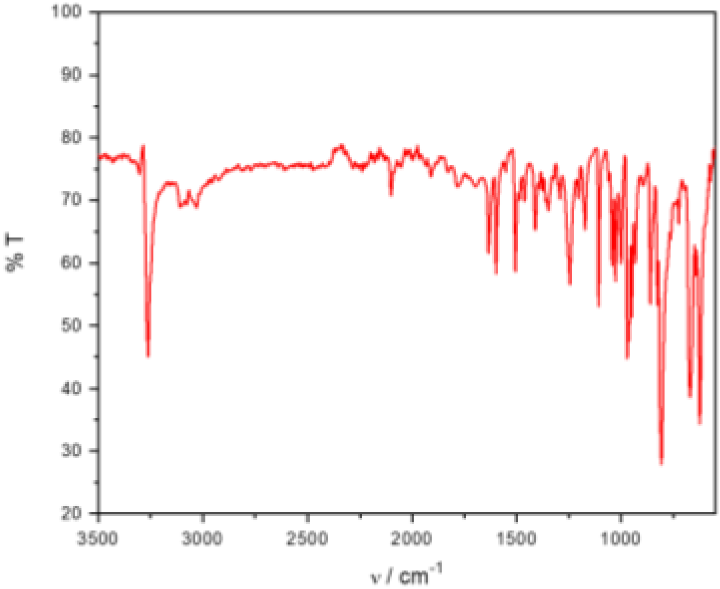

Fig. S14. FT-IR spectrum of compound ***trans*-1** in powder.

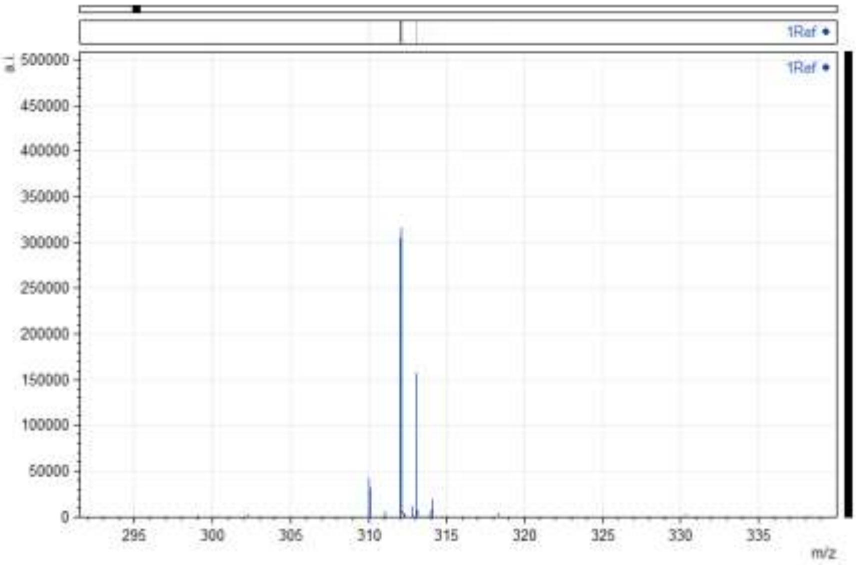

Fig. S15. Experimental LDI-ToF spectra of compound ***trans*-1**.

b) Compound ***cis*-1**

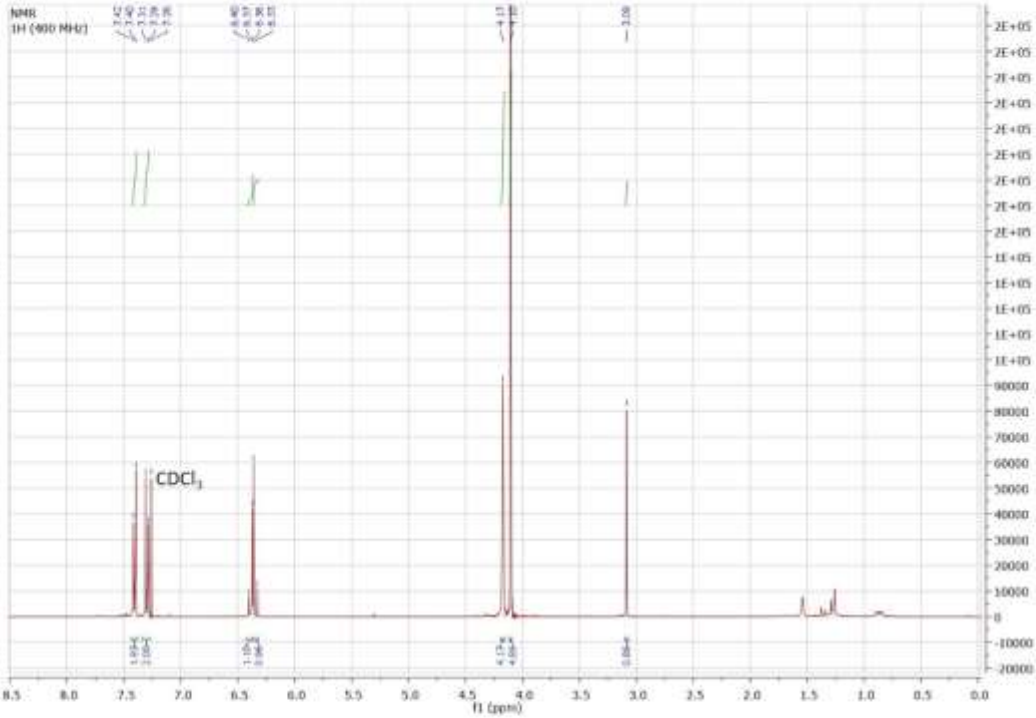

Fig. S16. ^{1}H-NMR spectrum of compound ***cis*-1** in $CDCl_3$.

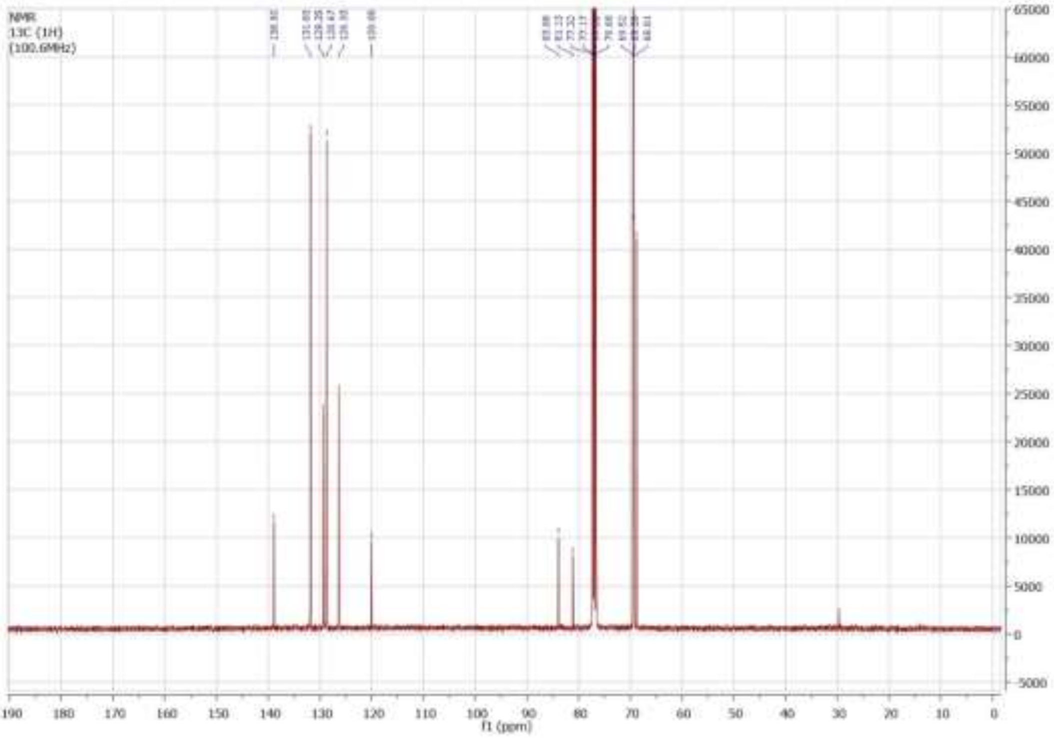

Fig. S17. ^{13}C-NMR spectrum of compound ***cis*-1** in $CDCl_3$

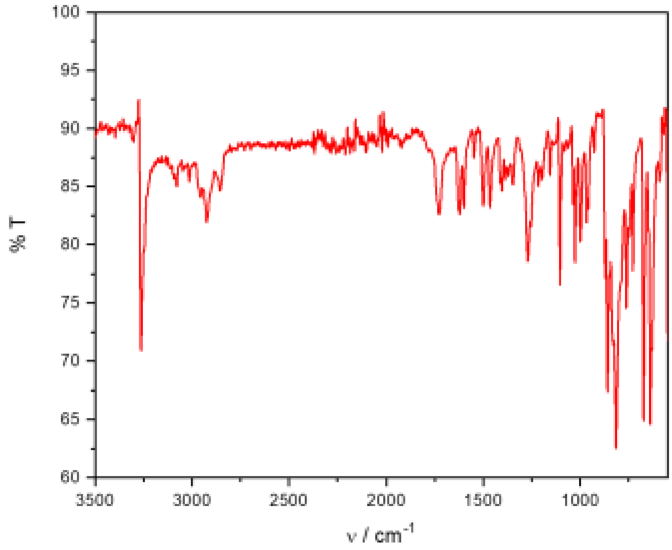

Fig. S18. FT-IR spectrum of compound ***cis*-1** in powder.

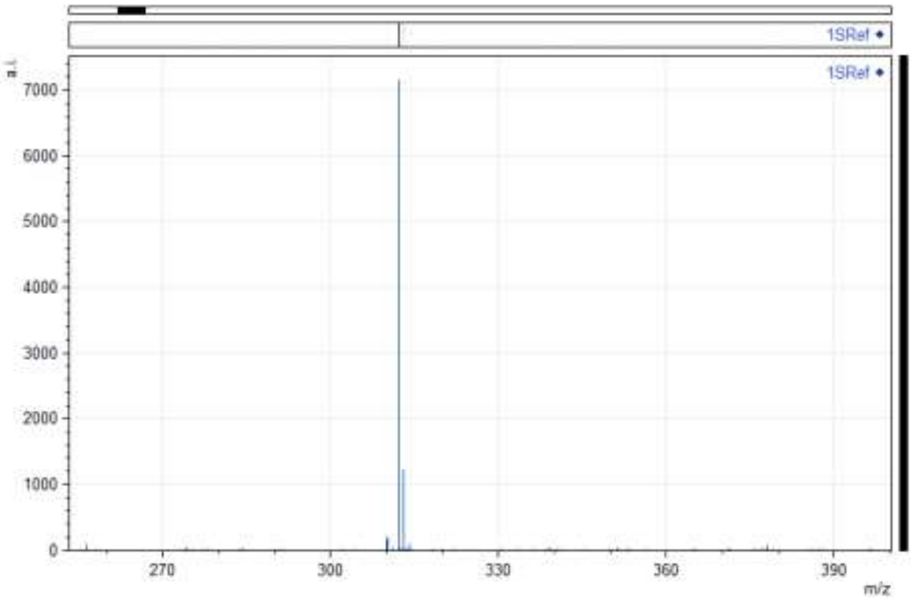

Fig. S19. Experimental LDI-ToF spectra of compound ***cis-1*.**